Phenotypic and molecular investigations on hypovirulent *Cryphonectria parasitica* in Italy

Sergio Murolo, Department of Agricultural, Food and Environmental Sciences, Marche Polytechnic University, Ancona, Italy; **Rita Milvia De Miccolis Angelini** and **Francesco Faretra**, Department of Soil, Plant and Food Sciences, University of Bari, Bari, Italy; **Gianfranco Romanazzi** Department of Agricultural, Food and Environmental Sciences, Marche Polytechnic University, Ancona, Italy

Key words: *Castanea sativa*, Chestnut blight, *Cryphonectria hypovirus 1*, hypovirulence, Illumina technology, molecular characterization

Corresponding author: Dr Sergio Murolo
Department of Agricultural, Food and Environmental Sciences
Marche Polytechnic University, Ancona, Italy
Tel: +39-071-2204697
Fax: +39-071-2204856
E-mail: s.murolo@univpm.it

Abstract

Murolo, S., De Miccolis Angelini, R.M., Faretra, F., Romanazzi, G. 2017. Phenotypic and molecular investigations on hypovirulent *Cryphonectria parasitica* in Italy. Plant Dis. XX:XX-XX.

Chestnut blight is caused by the fungus *Cryphonectria parasitica*. As one of the most ecologically important diseases of *Castanea* spp., *C. parasitica* can rapidly kill trees. In Europe, mitigation of disease severity took place spontaneously through colonization of *C. parasitica* by mycoviruses, which reduced the virulence of the fungus. In the framework of a survey, 138 *C. parasitica* isolates were identified, and virulent/hypovirulent phenotypes were determined through morphological properties and pathogenicity tests. For a pool of four hypovirulent isolates, dsRNA was extracted, cDNA synthesised, and a library subjected to next-generation sequencing. The bioinformatics analysis allowed detecting and reconstructing the complete genome of *Cryphonectria hypovirus 1* (CHV-1), denoted as CHV-1 Marche, as well excluding the presence of any other ssRNA and dsRNA viral sequence. When compared to the available genomes of other hypoviruses that affected the virulence of *C. parasitica*, available in databases, CHV-1 Marche showed some nucleotide diversity. The approach used in this study was effective to explore the virome inside a pool of hypovirulent *C. parasitica* isolates. In conclusion, next-generation sequencing allowed us to exclude the presence of any other ssRNA and dsRNA viruses infecting the fungus and determine CHV-1 as the only responsible of hypovirulence of *C. parasitica* in the analysed samples.

One of the most important and historical diseases of *Castanea* spp. is chestnut blight, which is caused by the Ascomycota fungus *Cryphonectria parasitica* (Murr) Barr (Rigling and Prospero 2017). This disease was first described in New York at the beginning of the last century. Then in Europe, *C. parasitica* was initially reported in 1938 in the Liguria region of Italy (Biraghi 1946), yet different introduction events were hypothesized to contribute to the current population structure as described by Dutech et al. (2010). Both in Italy and other areas in Europe, chestnut blight disease is less severe than for the North America (Robin and Heiniger 2001), in part because the European chestnut (*C. sativa* Mill.) is less susceptible than *C. dentata*, and in part due to a reduction in the virulence of *C. parasitica,* a phenomenon deeply studied by several researchers (Grente 1965; MacDonald and Fullbright 1991; Nuss 1992; Heiniger and Rigling 1994; Milgroom and Cortesi 2004). Recovery from chestnut blight has been observed in many European countries and in some areas of the United States, such as in Michigan (Milgroom and Cortesi 2004). In Europe, in particular, this recovery was ascribed to the presence of hypovirulent strains of *C. parasitica*, which was infected by *Cryphonectria hypovirus 1* (CHV-1) (Robin and Heiniger 2001). This prevalence of CHV-1 and the consequent induced hypovirulence of *C. parasitica* has most likely prevented the occurrence of devastating chestnut blight epidemics and the destruction of the European chestnut forests to date.

CHV-1 is a non-encapsidated cytoplasmic virus of the *Hypoviridae* family (Ghabrial et al. 2015). The phylogeny and time estimates suggest that CHV-1 was introduced into Italy together with *C. parasitica*, and spread across southern-central Europe and then eastern Europe (Bryner et al. 2012), due to the low genetic diversity of the *C. parasitica* populations. Indeed, CHV-1 can be horizontally transmitted through

hyphal anastomosis, which can occur efficiently between individual fungi that belong to the same vegetative compatibility group, but transmission can sometimes occur between genetically close vegetative compatibility types (Liu and Milgroom 1996). In the European regions where this natural hypovirulence did not appear, rapid dissemination of CHV-1 was further aided by active biocontrol efforts (Milgroom and Cortesi 2004). To date, chestnut blight incidence in Europe is high, but due to this hypovirulence, the disease is maintained at low severity in most regions (Milgroom and Cortesi 2004; Bryner et al. 2012, 2014).

CHV-1 infection leads to superficial swollen cankers (passive cankers), with reduced fungal growth and less sporulation, compared to active cankers (Milgroom and Cortesi 2004). However, a lack of any clear relationship between canker morphology and virus infection for *C. parasitica* was recently reported (Bryner et al. 2014). Hypovirus-infected *C. parasitica* isolates are often white in colour, and show reduced sporulation on potato dextrose agar growth medium, compared to non-infected isolates (Milgroom and Cortesi 2004). However, recently, blight damage recurrence has been reported for different European chestnut areas that are highly infested by the chestnut gall wasp (*Dryocosmus kuriphilus*), even in the presence of hypovirulent cankers (Meyer et al. 2015).

Starting from the evaluation of hypovirulent isolates of *C. parasitica* recovered from chestnut areas in the Marche and Abruzzi regions of Italy, where the damage of chestnut blight has been particularly mitigated, we applied next generation sequencing to investigate ssRNA and dsRNA mycoviruses and in particular to reconstruct the CHV-1 full-length genome, mainly involved in the hypovirulence.

Materials and Methods

Isolation and morphological characterisation. Within the framework of surveys carried out from 2013 to 2016 to determine the spread and severity of chestnut blight in the Marche and Abruzzi regions of Italy, cortical tissue from plants showing "active" (8 samples) and "passive cankers" (7 samples) were collected for each site, from plants approximately 10 m apart from each other.

Five bark samples per canker (i.e., one in the centre, four along the margins) were removed with a cork borer (diameter, 5 mm) that was sterilised with 95% ethanol solution during canker sampling. The bark disks were divided into two parts, which were placed into Petri dishes (diameter, 50 mm; two pieces/plate) containing water agar (Duchefa Biochimie, Haarlem, The Netherlands), and incubated for 3 days at 25±1°C in the dark. From the margin of each of the resulting fungal colonies, mycelial tips were collected and placed in Petri dishes containing potato dextrose agar (Duchefa Biochimie), with further subculturing in the same medium to obtain pure colonies. Each fungal isolate was stored in a glass tube containing potato dextrose agar at 4°C.

To characterize the morphological properties of each colony of *C. parasitica*, they were transferred to potato dextrose agar Petri dishes (diameter, 90 mm) and incubated for 7 days at 25±1°C in the dark. Fungal cultures were subsequently exposed to a photoperiod of 12 h for an additional 7 days, again at 25±1°C. These conditions are suitable for morphological characterisation of the *C. parasitica* isolates, and for distinguishing virulent colonies (orange mycelia, abundant pycnidia) from hypovirulent colonies (white mycelia, few or no pycnidia production) (Bissegger et al. 1997; Milgroom and Cortesi 2004).

Pathogenicity tests on chestnut cuttings. Based on the morphological characterisation 26 *C. parasitica* isolates (seven orange and 19 with white mycelium) representative of the surveyed areas were selected and tested for pathogenicity on excised dormant chestnut stems. The virulence of each isolate was determined on stems (diameter, 40-60 mm) from healthy *C. sativa* plants. The stems were cut into 50-cm-long segments and surface disinfected with an aqueous solution of 70% ethanol. The bark of the chestnut cuttings was removed every 15 cm using a cork borer (diameter, 5 mm); and each wound was inoculated with a *C. parasitica* mycelial disc (diameter, 5 mm), and then sealed with parafilm. As negative control we used PDA disks not inoculated (diameter, 5 mm). Three isolates were assayed per cutting, with three replicates for each set of isolates tested. Both ends of each cutting were covered with cottonwool soaked with water, and incubated in a plastic box, at 25°C under a 16-h photoperiod, for 10 days. The length and width of the necrotic areas of the cortical tissue and the wood were then measured with digital calipers (model 500-196-30; Mitutoyo America Corporation, Kanagawa, Japan) and the elliptical necrotic areas were calculated.

The means and standard deviations (sd) were calculated. These data were analysed statistically using one-way ANOVA, and the means were compared using Duncan's multiple range tests, at $P \leq 0.05$, using the Statistica package (Statsoft Inc., Tulsa, Oklahoma).

Re-isolations of *C. parasitica* was carried out directly from necrotic lesions of cortical and wood tissue, according to the procedure already mentioned in the previous paragraph.

DNA extraction and molecular characterisation of representative hypovirulent isolates. Based on morphological properties, pathogenicity, origin and year of collection, four hypovirulent isolates (i.e., P16_2, P29B, L25A, L2A) were selected for total DNA extraction, according to Varanda et al. (2016). The DNA was used in PCR reactions with the ITS1/ITS4 primers (White et al. 1990), and sequenced at the Beckman Coulter Facility (Essex, UK). The raw sequences were analysed by BLAST searches to look for sequence homology with other nucleotide sequences of *C. parasitica* available in Genbank (National Center for Biotechnology Information; NCBI). The vegetative compatibility of the selected isolates was also molecularly assessed according to Short et al. (2015).

dsRNA extraction. The same isolates of *C. parasitica* that were selected for total DNA extraction (i.e., P16_2, P29B, L25A, L2A) were tested for dsRNA. The isolates were inoculated in 40 ml Potato dextrose broth (Duchefa Biochimie), at 25°C for 10 days under agitation (150 rpm). The mycelia were collected by centrifugation at 3,840 × *g* for 15 min, then they were pressed between sterile sheets of paper for 24 h, and finally 10 g for each isolate were pulverised in liquid nitrogen. The dsRNA extraction was carried out according to Al Rwahnih et al. (2009). The dsRNA extracted was treated with 25 ng/ml RNase (Sigma Aldrich, Saint Louis, USA), 1 mg/ml DNase (Promega, Madison, USA) and 5 mg/ml proteinase K (Sigma Aldrich), to remove ssRNA, DNA, and protein, respectively. Aliquots of the purified dsRNA were run on 1% agarose gels, and images were acquired (Gel Doc XR; Bio-Rad, Hercules, USA).

Next-generation sequencing. Deep-sequencing of the extracted dsRNA samples was performed using Illumina technology. For library preparation, 800 ng dsRNA was subjected to heat denaturation (94°C for 12 min), and flash cooled in iced water. The fragmentation, conversion to cDNA, and preparation for sequencing was performed using TruSeqTM RNA Sample Prep v2 kits (Illumina, San Diego, USA).

After PCR enrichment (15 cycles), the adapter-ligated cDNA fragments were quantified, diluted to 12 pM, and hybridised to a flow cell for Illumina sequencing. Clusters on the flow cell were then generated using TruSeq SR Cluster Kit v3-cBot-HS (Illumina). The flow cells with the DNA clusters were subjected to sequencing using the Illumina platform (HiScanSQ System, SELGE Network Sequencing Service; http://www.selge.uniba.it/), using SBS Sequencing v3 kits to generate 50-bp single-end reads.

Bioinformatics analysis and reconstruction of the CHV genome. High-quality (quality score, ≥30) sequenced reads were filtered using Illumina Real-Time Analysis (RTA 1.13.48) and *de-novo* assembled using CLC Genomics Workbench 7.0.3 (CLC Bio, Qiagen, Hilden, Germany) with standard parameters, and Velvet 1.1.06, followed by Oases 0.2.8 with a minimum contig length of 100 nts, and a multiple K-mer approach (Zhao et al., 2011). SeqMan Pro (Lasergene v.10.1; DNASTAR, Inc., Madison, USA) was used for merging the resulting contigs. To search for homology to viral sequences, consensus sequences were subjected to BLASTN and BLASTX analysis against the NCBI database (www.ncbi.nlm.nih.gov), with the default parameters and the E-value cut-off of 10^{-3}. The contigs were then classified according to

the sequences with the highest bit score. Reference sequences were identified based on the BLAST results, and used in the subsequent analyses.

Transdecoder (https://transdecoder.github.io/) was used to identify open-reading frames (ORFs) and to select the best assembly for the putative mycoviral sequences. Subsequently, sequencing reads were mapped back to the reference sequences of CHV-1 and the *de-novo* assembled viral contigs, using SeqMan NGen and SeqMan Pro (Lasergene v.10.1; DNASTAR), to determine and correct miss-assembly errors, and to detect single nucleotide polymorphisms (SNPs).

Phylogenetic analysis. The consensus sequence identified as CHV-1 Marche was set up in FASTA format and aligned with the Clustal X software (Thompson et al. 1997), together with the nucleotide sequences of isolates CHV-1/EP-721 (Genbank accession number, DQ861913), CHV-1/EP713 (NC_001492), CHV-1/Euro7 (AF082191), and CHV-1/CN280 (KT726153). The phylogenetic tree was built using neighbour-joining in Molecular Evolution Genetic Analysis version 5 (MEGA5) (Tamura et al. 2011). The robustness of the tree topology was verified considering the bootstrap analysis (1000 replicates). In the phylogenetic analysis, other hypoviruses that can infect *C. parasitica* were considered as outgroups, in particular CHV-2 (NC_003534), CHV-3 (NC_000960) and CHV-4 (NC_006431), the complete genomes of which are available in the NCBI database.

Results

Morphological characterisation. From 150 samples of bark showing symptoms and signs of chestnut blight and collected in the framework of the surveys, 138 colonies of *C. parasitica* were recovered (Table 1). Using potato dextrose agar medium with a 12-h photoperiod at 25°C, majority of these isolates (85 out of 138) had orange mycelia and abundant pycnidia, and were thus recognized as virulent colonies (Fig. 1a). Fifty-three colonies, grew with white mycelia and only sporadic pycnidia in the central part of the colonies, were thus identified as hypovirulent (Fig. 1b).

Pathogenicity tests on chestnut cuttings. Significant differences were recorded between the *C. parasitica* virulent (orange) and hypovirulent isolates (white). The virulent isolates P4C4, P21A, P35D and PD1 produced the widest elliptical necrotic areas on both the bark and the wood (Table 2). Conversely, the hypovirulent isolates showed generally slow growth and smaller necrotic areas (Table 2). After 7 days, from the re-isolations of necrotic areas we obtained the corresponding virulent or hypovirulent isolates previously inoculated on the cuttings.

Molecular characterisation of representative hypovirulent isolates. The DNA extraction of the four selected hypovirulent *C. parasitica* isolates, P16_2, P29B, L25A and L2A, and the following amplification with the ITS1/ITS4 primer pair, yielded a specific band of ~600 bp, which showed high nucleotide homology with *C. parasitica* (Genbank accession number: KP824756). These four *C. parasitica* isolates belong to four different vegetative compatibility groups. Using multilocus PCR assays to assess *vic* genotype, P16_2 was confirmed molecularly as the vegetative compatibility

genotype 1112-11 (corresponding to EU12), P29B as 2112-11 (EU17), L25A as 2211-22 (EU5), and L2A as 2112-22 (EU2).

dsRNA extraction. The dsRNA was extracted from a pool of the same four *C. parasitica* isolates, P16_2, P29B, L25A and L2A, which showed similar morphologies and virulence but that were isolated from different locations. Only one band of 12,000 bp in size corresponding to L-dsRNA was obtained. No bands were visualised on the gels for P4C4, P21A, P35D and PD1, representative virulent isolates of *C. parasitica* that were analysed.

Sequencing and bioinformatics analysis of mycoviruses. The dsRNA was prepared for cDNA synthesis and library construction, followed by sequencing. A total of 19,068,188 short reads were initially generated in this study, which resulted in ~1 Gb of raw sequencing data [submitted in the NCBI Sequence Read Archive (SRA) database with submission number SUB2316937]. There were 626,078 non-redundant reads. After filtering, only the high-quality reads (quality score, ≥30) were considered for further analysis. To detect and identify putative mycoviral sequences in the selected isolates of *C. parasitica*, the reads were submitted to *de-novo* assembly and analysis of the assembled contigs. CLC Genomics Workbench assembler produced 239 contigs, which included many small sequences of <1 kb in length. Among the largest contigs, four that were 619, 2,015, 3,251, and 6,233 nts in length together contained 98.6% of the assembled reads and were identified as partial non-overlapping sequences of the *Cryphonectria hypovirus 1* (CHV-1) genome (12,724 nts; Genbank accession number, DQ861913). Velvet, followed by Oases for the *de-novo* RNA-Seq assembly were used

to assemble the complete viral genome from the reads into a single contig. Most of the contigs produced at different k-mer values (i.e., 37-21), which ranged between 451 and 591, were clearly overlapping and showing only small differences in their sequences.

The largest assembled sequence (13,013 bp) that shared the highest sequence identity with the CHV-1 genome and the best candidate coding regions within its sequence was selected as the template for realignment of the reads and for manual curation. The complete viral genome of the CHV-1 that infects *C. parasitica* isolates from the Marche region in Italy (CHV-1_Marche) was conclusively obtained and has been submitted to GenBank (Accession number, KY471627). This is 12,735 nts in length, has a sequence identity of 98% with CHV-1 (i.e., DQ861913, AF082191) (E-value, 0.0), and contains two putative ORFs of 622 and 3,164 amino acids, both with 99% amino-acid identity to the two polyproteins identified as ORFA (ABI64295.1) and ORFB (ABI64296.1), respectively, in CHV-1. A total of 18,664,706 viral reads (97.9% of the total reads) was mapped to the genome consensus sequence, with an average coverage of 82,223×. The read depth was enough to obtain some preliminary data on the viral diversity in the analysed CHV-1 population from this pool of four *C. parasitica* isolates. Single nucleotide variants were identified by applying a read depth threshold of 50, with these recognized as putative SNPs when present in at least 20% of the reads (Supplemental Material Table S1). Out of the 125 nucleotide substitutions detected throughout the CHV-1 genome, 106 (84.8%) were conservative (pyrimidine to pyrimidine, or purine to purine). In detail, four SNPs were identified outside the coding regions, and of the remaining SNPs, 77 (61.6%) were synonymous or silent substitutions that did not affect the protein sequence, while 44 resulted in amino-acid changes in the ORFA (11) and ORFB (33) polyproteins.

Phylogenetic analysis. The phylogenetic analysis carried out using the MEGA 5 software included the CHV-1 Marche genome (KY471627) in the cluster with the other CHV-1 genomes of European and Asiatic origin, which are phylogenetically different (as demonstrated by the bootstrap values) from the other *Hypovirus* (i.e., CHV-2, CHV-3, CHV4) that can infect *C. parasitica* (Fig. 2).

Discussion

Chestnut blight is common in the Marche region, where its incidence ranging from 20% to 60%. The severity of the symptoms appears to be related to the age of the plants, and mostly to the silvicultural practices adopted (Amorini et al. 2001). In some situations, the severity of decline in chestnut is related to the infestation of the chestnut gall wasp (Meyer et al. 2015). During these surveys carried out from 2013 to 2016, *C. parasitica* was isolated and identified in about 90% of the bark samples.

Most of these isolates (i.e., 85 out of 138) were virulent, they showed typical morphological features, and they resulted in wide necrotic areas during the pathogenicity tests. These were isolated from active cankers, on which perithecia were sporadically identified. In Europe, the production of perithecia has been observed in several countries, including Italy, although at medium to low frequency (Prospero and Rigling 2013). On the other hand, 53 hypovirulent *C. parasitica* isolates were obtained and characterised by white mycelia, reduced colony growth, and differentiation of few pycnidia. As demonstrated in previous investigations, these anomalies are caused by viruses that can infect *C. parasitica*, which can induce several phenotypic changes in this fungus, such as a reduction in asexual sporulation, inhibition of sexual

304 reproduction, altered colony morphology, and reduced pigmentation (Nuss 2005).
305 Mycovirus-induced hypovirulence has been reported not only in *C. parasitica*, but also
306 in *Ophiostoma ulmi*, *Ophiostoma novo-ulmi*, *Botrytis cinerea*, *Sclerotinia sclerotiorum*,
307 *Sclerotinia homoeocarpa* and *Rosellinia necatrix* (Ghabrial et al. 2015).
308 The *C. parasitica* hypovirulent isolates P16_2, P29B, L25A and L2A were chosen as
309 representative isolates and next submitted to more detailed molecular characterisation.
310 Molecular identification according to the analysis of internal transcribed spacer (ITS)
311 nucleotide sequences confirmed the identity of these fungal isolates. In particular, the
312 ITS region appeared appropriate for molecular identification and to establish the
313 phylogenetic relationships, even with closely related fungal species (Myburg et al.
314 2004).

315 To determine the vegetative incompatibility gene profiles of the selected isolates
316 of *C. parasitica*, multilocus PCR assays were carried out, as described by Short et al.
317 (2015). This new approach is in agreement with the genetically determined vegetative
318 incompatibility genotypes (Cortesi and Milgroom 1998), and it is generally equivalent
319 to the culture-dependent assays. These culture-dependent assays are time consuming
320 and require well-maintained in-house EU tester strains, and they are not always easy
321 when interpreting barrage reactions (Short et al. 2015). These *C. parasitica* isolates that
322 originated in Marche show four main vegetative incompatibility genotypes that
323 correspond to the vegetative compatibility groups EU12, EU17, EU5 and EU2.

324 L-dsRNA (~12 kb) was detected in all the four hypovirulent *C. parasitica*
325 isolates, which is complete replicative form. M-dsRNA (8-10 kb) and S-dsRNA (0.6-1.7
326 kb), which represent deleted forms of L-dsRNA that can persist during replication
327 (Montenegro et al. 2008) were not found. To date, mycoviruses have commonly been

328 detected following the isolation of their dsRNA. Today, NGS has become feasible to
329 use as whole-genome and metagenomics (Mokili et al. 2012) approaches, to screen
330 fungi for the presence of potential novel viruses. Recently, Schoebel et al. (2014)
331 detected mycoviruses in the plant pathogenic fungus *Hymenoscyphus fraxineus* through
332 a combination of NGS with bioinformatics.

333 The approach used in the present study involved dsRNA isolation and
334 fragmentation, and cDNA library preparation, with Illumina-based sequencing, *de-novo*
335 assembly, and identification of putative sequences of ssRNA and dsRNA virus. This
336 was effective and accurate to determine the virome inside a pool of hypovirulent
337 isolates of *C. parasitica*.

338 To the best of our knowledge, this is the first time that the CHV-1 genome has
339 been reconstructed by NGS, and the quality is comparable to that of sequence genomes
340 obtained by the Sanger method and available in the NCBI database. Indeed, Kalifa et al.
341 (2016) recently demonstrated that the accuracy of the sequences obtained using the
342 Illumina platform is comparable with Sanger sequencing analysis. Moreover, to
343 enhance the accuracy of the Illumina analysis, we started from purified dsRNA, to
344 maximise the proportion of viral sequences in the data, while using sufficiently rigorous
345 quality controls, and maintaining the level of depth and coverage of the sequencing
346 data.

347 In this situation, we started from a pool of four isolates that shared
348 morphological characteristics and virulence, but were collected from different locations
349 within the Marche region, and only the viral genome of CHV-1 was detected. It is
350 known that *C. parasitica* can be the host of several hypoviruses, reoviruses, and
351 crysoviruses (Ghabrial et al. 2015). From the phylogenetic analysis, it was clear that

352 CHV-1_Marche is in the same cluster with the other CHV-1 genomes available in the
353 NCBI database. In particular, CHV-1 Marche belongs to subtype I, as well as CHV-
354 1/EP721 and CHV-1/Euro 7, whose origin is Italy. It is slightly divergent from CHV-
355 1/EP713 belonging to subtype F1, whose origin is France and more consistently
356 different from CHV-1/CN280 belonging to subtype CN6, whose origin is China (Du et
357 al. 2017). On the other hand, CHV-1 Marche is clearly different from other hypoviruses
358 that can infect *C. parasitica*, and in particular, CHV-2, CHV-3 and CHV-4. It was
359 interesting to observe that CHV-2 is the hypovirus closest to CHV-1 and they have
360 similar genome lengths. Conversely, CHV-3 and CHV-4 are genetically more distant,
361 because they have shorter genomes (by about 9 kbp) and cause lower degrees of
362 hypovirulence (Ghabrial et al. 2015).

363 The simplicity of the sample composition here allowed more detailed sequence
364 analysis, which revealed interesting genetic diversity inside the analysed pool, although
365 the origin is restricted. A wider genetic diversity was recorded by Feau et al. (2014),
366 who analysed several samples belonging to different CHV-1 subtypes and whose
367 origins were different. Our study confirmed that in Italy, and in particular in Marche
368 region, CHV-1 subtype I is the only recorded, as well as in other European Countries
369 (Croatia, Greece, Hungary, Macedonia, Slovenia, Switzerland) (Allemann et al. 1999;
370 Prospero and Rigling 2013). On the other hand, different CHV-1 subtypes were
371 recorded in Spain (D, E, F1, I) (Montenegro et al. 2008; Trapiello et al. 2017) and
372 France (F1, F2, I) (Feau et al. 2014), where a multiple introduction of hypovirulence
373 was hypothesised.

374 Moreover, in the present study, the genetic diversity is more related to silent
375 substitutions (81), although these also include SNPs (44) causing amino-acid

substitutions in the two coding regions of the CHV-1 genome (i.e., ORFA, ORFB). The intraspecific variability that was recorded for the pool of four isolates is very common for RNA viruses, which are characterised by complex evolutionary dynamics, high mutation rates, and rapid replication kinetics. Moreover, the presence of silent and non-silent substitutions in ORFA and ORFB might be the result of the interactions between the CHV-1 genome and *C. parasitica*. In particular, viruses have counter-measures to escape host antiviral responses. Many RNA silencing suppressors that target different silencing stages have been reported, and these are diverse in their amino-acid sequences and protein structures (Segers et al. 2006). Like pathogenic viruses of mammals, insects and plants, hypoviruses also encode protein suppressors of RNA interference. The papain-like protease p29 that is encoded by CHV-1 functions as a suppressor of RNA silencing in the natural fungal host (Segers et al. 2006).

In conclusion, the application of NGS is a valid and accurate tool to explore the virome of *C. parasitica* hypovirulent isolates, to analyse the full-length genome of CHV-1 and to exclude the presence of additional ssRNA and dsRNA mycoviruses potentially involved in the hypovirulence.

Acknowledgements

This study was supported by Marche Polytechnic University through the projects "Diagnosis of emergent disease agents in forest plant" and "Hypovirulence and *Cryphonectria parasitica*". We thank Prof. Paolo Cortesi and Prof. Michael Milgroom for providing EU testers (EU reference strains). We are grateful to A. Corvaro, L.

399 Marchegiani, A. Moresi, A. Servili, G. Millozzi, G. Girolami and A. Santini for
400 assistance during the surveys and the collection of samples.

Literature Cited

Allemann, C., Hoegger, P., Heiniger, U., and Rigling, D. 1999. Genetic variation of *Cryphonectria* hypoviruses (CHV1) in Europe, assessed using restriction fragment length polymorphism (RFLP) markers. Mol. Ecol. 8:843-854.

Al Rwahnih, M,, Daubert, S., Golino, D., and Rowhani, A. 2009. Deep sequencing analysis of RNAs from a grapevine showing Syrah decline symptoms reveals a multiple virus infection that includes a novel virus. Virology 387: 395-401.

Amorini, E., Manetti, M.C., Turchetti, T., Sansotta, A., and Villani, F. 2001. Impact of silvicultural system on *Cryphonectria parasitica* incidence and on genetic variability in a chestnut coppice in Central Italy. Forest Ecol. Manag.142:19-31.

Biraghi, A. 1946. Il cancro del castagno causato da *Endothia parasitica*. L'Italia Agricola 7:406.

Bissegger, M., Rigling, D., and Heininger, U. 1997. Population structure and disease development of *Cryphonectria parasitica* in European chestnut forests in the presence of the natural hypovirulence. Phytopathology 87:50-59.

Bryner, S.F., Prospero, S., and Rigling, D., 2014. Dynamics of *Cryphonetria hypovirus* infection in chestnut blight cankers. Phytopathology 104:918-925.

Bryner, S.F., Rigling, D., and Brunner, P.C. 2012. Invasion history and demographic pattern of *Cryphonectria hypovirus* 1 across European populations of the chestnut blight fungus. Ecol. Evol. 2:3227-3241.

Cortesi, P., and Milgroom, M.G. 1998. Genetics of vegetative incompatibility in *Cryphonectria parasitica*. Appl. Environ. Microbiol. 64:2988-2994.

424 Du, Y, Lin, Y, Zhou, X, Wang, K, Fang, S, Deng, Q. 2107. Full-length sequence and
425 genome analysis of CHV1-CN280, a North China isolate of Cryphonectria
426 hypovirus 1. Arch. Virol. 162(6):1811-1818.
427 Dutech, C., Fabreguettes, O., Capdevielle, X., and Robin, C. 2010. Multiple
428 introductions of divergent genetic lineages in an invasive fungal pathogen,
429 Cryphonectria parasitica, in France. Heredity 105:220-228.
430 Feau, N., Dutech, C., Brusini, J., Rigling, D., and Robin, C. 2014. Multiple
431 introductions and recombination in *Cryphonectria hypovirus* 1: perspective for a
432 sustainable biological control of chestnut blight. Evol. Appl. 7:580-596.
433 Ghabrial, S.A., Castón, J.R., Jiang, D., Nibert, M.L., and Suzuki, N. 2015. 50-plus years
434 of fungal viruses. Virology 479:356-368.
435 Grente, J. 1965. Les formes hypovirulentes d'Endothia parasitica et les spoirs de lutte
436 contre le chancre du châtaignier. Comptes-rendus des Seances de l'Academie
437 d'Agriculture de France 51:1033-1037.
438 Heiniger, U., and Rigling, D. 1994. Biological control of chestnut blight in Europe.
439 Annu. Rev. Phytopathol. 32:581-599.
440 Khalifa, M.E, Varsani, A., Ganley, A.R., and Pearson, M.N. 2016. Comparison of
441 Illumina de *novo* assembled and Sanger sequenced viral genomes: A case study
442 for RNA viruses recovered from the plant pathogenic fungus *Sclerotinia*
443 *sclerotiorum*. Virus Res. 219:51-57.
444 Liu, Y.C., and Milgroom, M.G. 1996. Correlation between hypovirus transmission and
445 the number of vegetative incompatibility (*vic*) genes different among isolates
446 from a natural population of *Cryphonectria parasitica*. Phytopathology 86:79-
447 86.

448 MacDonald, W. L., and Fullbright, D. W. 1991. Biological control of chestnut blight:
449 Use and limitations of transmissible hypovirulence. Plant Dis. 75:656-661.
450 Meyer, J., Gallien, L., and Prospero, S. 2015. Interaction between two invasive
451 organisms on the European chestnut: does the chestnut blight fungus benefit
452 from the presence of the gall wasp? FEMS Microbiol. Ecol. 91:fiv122 (doi:
453 10.1093/femsec/fiv12210.1093/femsec/fiv122).
454 Milgroom, M.G., and Cortesi, P. 2004. Biological control of chestnut blight with
455 hypovirulence: a critical analysis. Annu. Rev. Phytopathol. 42:311-338.
456 Mokili, J.L., Rohwer, F., and Dutilh, B.E. 2012. Metagenomics and future perspectives
457 in virus discovery. Curr Opin Virol. 2:63-77.
458 Montenegro, D., Aguín, O., Sainz, M., Hermida, M., and Mansilla, J. 2008. Diversity of
459 vegetative compatibility types, distribution of mating types and occurrence of
460 hypovirulence of *Cryphonectria parasitica* in chestnut stands in NW Spain.
461 Forest Ecol. Manag. 256:973-980.
462 Myburg, H., Gryzenhout, M., Stipes, R.J., and Wingfield, M.J. 2004. Phylogenetic
463 relationships of *Cryphonectria* and *Endothia* species, based on DNA sequence
464 data and morphology. Mycologia 96:990-1001.
465 Nuss, D. L. 1992. Biological control of chestnut blight: An example of virus-mediated
466 attenuation of fungal pathogenesis. Microbiol. Rev. 56:561-576.
467 Nuss, D.L. 2005. Hypovirulence: mycoviruses at the fungal-plant interface. Nature
468 Reviews Microbiology 3:632-642.
469 Prospero, S., and Rigling, D. 2013. Chestnut blight. In G. Nicolotti & P. Gonthier
470 (Eds.), *Infectious Forest diseases* (pp. 318–39). Wallingford, UK: CAB
471 International.

472 Rigling, D., and Prospero, S. 2017. Cryphonectria parasitica, the causal agent of
473 chestnut blight: Invasion history, population biology and disease control. Mol.
474 Plant. Pathol. (DOI: 10.1111/mpp.12542).
475 Robin, C., and Heiniger, U. 2001. Chestnut blight in Europe: diversity of *Cryphonectria*
476 *parasitica*, hypovirulence and biocontrol. For. Snow Landsc. Res. 76:361-367.
477 Schoebel, C.N., Zoller, S., and Rigling, D., 2014. Detection and genetic characterization
478 of novel mycovirus in *Hymenoscyphus fraxineus*, the causal agent of ash
479 dieback. Infect. Genet. Evol. 28:78-86.
480 Segers, G.C., Wezel, R.V., Zhang, X., Hong, Y., and Nuss, D.L. 2006. Hypovirus
481 papain-like protease p29 suppresses RNA silencing in the natural fungal host
482 and in a heterologous plant system. Eukaryot. Cell 5:896-904.
483 Short, D.P., Double, M., Nuss, D.L., Stauder, C.M., MacDonald, W., and Kasson, M.T.
484 2015. Multilocus PCR assays elucidate vegetative incompatibility gene profiles
485 of *Cryphonectria parasitica* in the United States. Appl. Environ. Microbiol.
486 81:5736-5742.
487 Tamura, K., Peterson, D., Peterson,N., Stecher, G., Nei, M., and Kumar, S. 2011.
488 MEGA5: Molecular Evolutionary Genetics Analysis using Maximum
489 Likelihood, Evolutionary Distance, and Maximum Parsimony Methods. Mol.
490 Biol. Evol. 28:2731-2739.
491 Thompson, J.D., Gibson, T.J., Plewniak, F., Jeanmougin, F., and Higgins, D.G. 1997.
492 The CLUSTAL_X windows interface: flexible strategies for multiple sequence
493 alignment aided by quality analysis tools. Nucleic Acids Res. 25:4876-4882.
494 Trapiello, E., Rigling, D., and Gonzalez, A.J. 2017. Occurrence of hypovirus- infected
495 *Cryphonectria parasitica* isolates in northern Spain: an encouraging situation for

biological control of chestnut blight in Asturian forests. Eur. J. Plant Pathol. (DOI 10.1007/s10658-017-1199-4).

Varanda, C.M.R., Oliveira, M., Materatski, P., Landum, M., Clara, M.I.E., and Felix, M.R. 2016. Fungal endophytic communities associated to the phyllosphere of grapevine cultivars under different types of management. Fungal Biol. 120:1525-1536.

White, T.J., Bruns, T., Lee, S., and Taylor, J. 1990. Amplification and direct sequencing of fungal ribosomal RNA genes for phylogenetics. In: Innis MA, Gelfand DH, Sninsky JJ, White TJ, eds. *PCR Protocols: a Guide to Methods and Applications*. Academic Press, New York, pp. 315–322.

Zhao, Q.Y., Wang, Y., Kong, Y.M., Luo, D., Li, X., Hao, P., 2011. Optimizing *de novo* transcriptome assembly from short-read RNA-Seq data: a comparative study. BMC Bioinformatics 12(14):S2. 10.1186/1471-2105-12-S14-S2.

Table 1. Morphological features associated with virulent (V) and hypovirulent (H) *Cryphonectria parasitica* isolates collected during the surveys from 2013 to 2016.

Region	Location	Isolates	n. isolates	Morphological features associated with V and H *C. parasitica*	Year of collection
Marche	Montemonaco (AP)	P1, P2, P3, P4, P4C4, P7, P8, P9, P11, P13b PA2, PD1	12	V	2013
		P3B, P4C2, P5, P6D, P6C, P10C, P11C, P12, P13A, PA1, PC	11	H	
	Rotella (AP)	P14, P15, P16, P17, P18, P19C	6	V	2013
		P14-1, P16_2, P19A, P20	4	H	
	Colle San Marco (AP)	P40, P41, P42, P44	4	V	2013
		P40B, P43	2	H	
	Colle, Ascoli Piceno	L24b, L24a, L26A	3	V	2015
		L25A, L26B	2	H	
	San Gregorio, Ascoli Piceno	D3A, D4A	2	V	2016
		D1A, D2B, D6B, D9B, D4B, L2A	6	H	
	Montefortino (AP)	P29c, P30, P31A	3	V	2013
		P28b, P29B, P30D	3	H	
	Collefalciano, Acquasanta Terme (AP)	P21A, P22B, P23, P25B, P26, P27	6	V	2013
		P21C, P22A, P24, P25	4	H	
	Pozza, Acquasanta Terme (AP)	L16A, L16b, L17A, L17b, L18b, L18 E4A, E6A, E8 B	9	V	2015 2016
		E2B, E3B, E7B bis	3	H	2016

	Umito, Acquasanta Terme (AP)	L19a, L19B, L20, L21a A3A, A4B, A8A, A9A, A15B	9	V	2015 2016
		L21b, L22A, L22b A2A, A5C, A6A, A7A, A10B	8	H	2015 2016
	Colle Frattale, Acquasanta Terme (AP)	L27a, L28A, L29a	3	V	2015
		L28c	1	H	
	Rocca di Montecalvo, Acquasanta Terme (AP)	C5B, C6A	2	V	2016
		C3B, C4A	2	H	
Abruzzi	Teramo (TE)	P33, P34, P35D, P36, P38, P39	6	V	2013
		P32, P37A1, P38A2	3	H	
	Pianaccio, Valle Castellana (TE)	L1a, L1c, L3a, L4, L5a, L5b, L6A, L6b, L7	9	V	2014
	Morrice, Valle Castellana (TE)	L8, L9A, L9b, L10c, L11, L12a, L13a, L13b, L15a, L15b	10	V	2014
		L14A	1	H	
	Valle Castellana (TE)	B3B	1	V	2016
		B5B, B6B, B9B	3	H	

Table 2. *Cryphonectria parasitica* isolates used in the pathogenicity tests with chestnut cuttings.

Isolate	Morphological features	Cortical necrotic area (mean ±sd; cm^2)	Wood necrotic area (mean ±sd; cm^2)
P4C4	Orange	7.3 ± 0.3 a	10.2 ± 0.6 a
P21A	Orange	6.5 ± 1.1 bc	7.0 ± 1.3 b
PD1	Orange	5.4 ± 0.5 de	6.8 ± 0.2 b
P35D	Orange	6.9 ± 2 b	6.3 ± 1.8 b
P31A	Orange	4.4 ± 1.1 e-g	5.1 ± 1.4 c
P22B	Orange	5.3 ± 0.7 cd	5.0 ± 0.5 c
P10C	White	4.4 ± 0.6 ef	4.0 ± 0.6 d
P14-1	White	3.4 ± 0.3 f-i	3.5 ± 0.5 de
P40B	White	3.7 ± 1.1 f-h	3.4 ± 1 d-f
P13A	White	2.8 ± 0.5 f-l	2.8 ± 0.8 d-g
PC	White	2.3 ± 0.5 l-n	2.7 ± 0.7 e-h
P16_2	White	2.9 ± 0.2 g-l	2.5 ± 0.1 e-h
P6C	White	2.7 ± 0.8 h-m	2.5 ± 0.7 e-h
P19A	White	2.6 ± 0.6 h-n	2.5 ± 0.7 e-h
P25	White	2.5 ± 0.2 h-n	2.5 ± 0.3 e-h
P9	Orange	2.6 ± 1 h-n	2.4 ± 0.8 e-h
P38A2	White	2.4± 0.5 h-n	2.3 ± 0.8 f-h
P43	White	2.2 ± 0.1 i-n	2.3 ± 0.5 e-h
P12	White	2.6 ± 0.2 h-n	2.2 ± 0.3 f-h
P30D	White	2.5 ± 0.7 h-n	2.2 ± 0.6 f-h
P29B	White	2.4 ± 0.5h-n	2.1 ± 0.6 gh
P11C	White	2.3 ± 1 i-n	2.1 ± 0.9 gh
L25A	White	2.3 ± 0.7 i-n	2.0 ± 0.6 gh
PA1	White	1.8 ± 0.3 l-o	1.6 ± 0.2 hi
P41	White	1.4 ± 0.3 n-o	1.5 ± 0.1 hi
L2A	White	1.5 ± 0.2 m-o	1.4 ± 0.4 hi

Data followed by different letters are significantly different (Duncan's multiple range tests; $P < 0.05$).

Table S1. Single nucleotide polymorphisms detected in the CHV-1_Marche genome by analysis of Illumina reads.

Nucleotide position (genome)	ORF	Nucleotide position (ORF)	Consensus base	Variant base	Depth at SNP	SNP (%)	Codon position	Codon change	Amino-acid change	SNP
149	-	-	T	G	6202	26.0	-	-	-	nc
415	-	-	T	C	7812	44.1	-	-	-	nc
579	A	85	A	G	4398	45.0	29	AGG/GGG	R/G	ns
594	A	100	G	A	2301	31.7	34	GTC/ATC	V/I	ns
1124	A	630	C	T	1242	26.2	210	GTC/GTT	V/V	s
1152	A	658	A	C	2240	32.8	220	ACC/CCT	T/P	ns
1154	A	660	C	T	2290	29.8	220	ACC/CCT	T/P	ns
1190	A	696	C	T	1170	36.2	232	TAC/TAT	Y/Y	s
1197	A	703	G	A	644	35.7	235	GTT/ATT	V/I	ns
1253	A	759	G	A	232	28.0	253	CCG/CCA	P/P	s
1304	A	810	T	C	78	23.1	270	ACT/ACC	T/T	s
1350	A	856	A	G	259	39.0	286	AGT/GGT	S/G	ns
1357	A	863	C	T	258	20.9	288	ACC/ATC	T/I	ns
1489	A	995	A	G	415	24.3	332	TAC/TGC	Y/C	ns
1583	A	1089	A	G	1115	41.3	363	GTA/GTG	V/V	s
1709	A	1215	C	T	312	26.6	405	AGC/AGT	S/S	s
1830	A	1336	A	G	233	49.8	446	AAA/GAA	K/E	ns
1956	A	1462	T	C	2009	36.2	488	TTT/CTT	F/L	ns
2087	A	1593	A	C	652	23.8	531	CAA/CAC	Q/H	ns
2165	A	1671	G	T	1447	34.3	557	GCG/GCT	A/A	s
2186	A	1692	G	A	3470	38.0	564	CGG/CGA	R/R	s
2249	A	1755	T	C	14436	25.1	585	TAT/TAC	Y/Y	s
2444	B	82	G	C	15539	23.0	28	GCG/CCG	A/P	ns

2710	B	348	C	T	37141	49.8	116	GGC/GGT	G/G	s
2828	B	466	C	T	22239	30.8	156	CTA/TTA	L/L	s
2929	B	567	G	A	4106	28.1	189	CCG/CCA	P/P	s
2932	B	570	A	G	3219	27.7	190	ACA/ACG	T/T	s
2944	B	582	C	A	3181	20.5	194	GGC/GGA	G/G	s
2947	B	585	C	A	3216	29.4	195	ATC/ATA	I/I	s
3045	B	683	C	T	3285	33.1	228	ACC/ATC	T/I	ns
3090	B	728	A	C	2190	25.1	243	AAG/ACG	K/T	ns
3328	B	966	C	T	4310	24.1	322	AGC/AGT	S/S	s
3447	B	1085	G	A	409375	20.2	362	AGG/AAG	R/K	ns
3622	B	1260	G	A	304634	30.4	420	GAG/GAA	E/E	s
3764	B	1402	C	T	68550	20.2	468	CCT/TCT	P/S	ns
3891	B	1529	A	G	2285	26.0	510	CAC/CGC	H/R	ns
3970	B	1608	C	T	2781	20.2	536	CCC/CCT	P/P	s
3973	B	1611	G	A	2772	32.8	537	GTG/GTA	V/V	s
3998	B	1636	T	C	3926	43.0	546	TAT/CAT	Y/H	ns
4022	B	1660	A	G	2352	23.3	554	AAG/GAG	K/E	ns
4048	B	1686	A	G	2449	45.9	562	TCA/TCG	S/S	s
4198	B	1836	A	G	2154	22.7	612	CGA/CGG	R/R	s
4286	B	1924	A	G	2391	38.8	642	AAT/GAT	N/D	ns
4416	B	2054	A	G	1126	23.4	685	GAC/GGC	D/G	ns
4441	B	2079	A	G	1354	45.4	693	GTA/GTG	V/V	s
4501	B	2139	T	C	2289	25.3	713	CCT/CCC	P/P	s
4580	B	2218	T	G	54188	22.9	740	TCG/GCG	S/A	ns
4633	B	2271	C	A	28624	28.5	757	ATC/ATA	I/I	s
4789	B	2427	A	T	119037	48.3	809	GTA/GTT	V/V	s
4796	B	2434	C	A	121257	43.0	812	CTC/ATC	L/I	ns
4834	B	2472	A	G	40584	49.5	824	ATA/ATG	I/M	ns
4837	B	2475	G	A	40553	25.1	825	TTG/TTA	L/L	s
4846	B	2484	C	A	37690	39.6	828	CCC/CCA	P/P	s

4924	B	2562	A	G	30861	20.5	854	GAA/GAG	E/E	s
4956	B	2594	A	G	21513	48.9	865	AAT/AGC	N/S	ns
4957	B	2595	T	C	21533	20.0	865	AAT/AGC	N/S	ns
5068	B	2706	T	C	12679	48.1	902	GTT/GTC	V/V	s
5551	B	3189	T	C	10758	25.9	1063	GGT/GGC	G/G	s
6261	B	3899	C	T	26097	42.5	1300	CCC/CTC	P/L	ns
6304	B	3942	G	A	31456	36.4	1314	GCG/GCA	A/A	s
6430	B	4068	A	G	16830	25.1	1356	GCA/GCG	A/A	s
6494	B	4132	G	A	804	24.4	1378	GCC/ACC	A/T	ns
6646	B	4284	G	A	120723	40.9	1428	CGG/CGA	R/R	s
6846	B	4484	A	C	65736	30.1	1495	GAA/GCA	E/A	ns
6882	B	4520	T	A	39115	29.3	1507	GTC/GAC	V/D	ns
6903	B	4541	A	G	21120	29.0	1514	GAC/GGC	D/G	ns
6915	B	4553	A	G	27128	39.9	1518	AAG/AGG	K/R	ns
6977	B	4615	A	G	17405	23.6	1539	AAC/GAC	N/D	ns
6997	B	4635	A	G	3908	41.5	1545	TTA/TTG	L/L	s
7003	B	4641	C	T	3693	22.7	1547	GGC/GGT	G/G	s
7077	B	4715	C	T	12677	34.6	1572	TCG/TTG	S/L	ns
7129	B	4767	A	G	9554	44.6	1589	CTA/CTG	L/L	s
7158	B	4796	A	C	13123	39.7	1599	AAC/ACC	N/T	ns
7366	B	5004	A	G	46370	38.5	1668	CCA/CCG	P/P	s
7409	B	5047	G	A	5347	25.3	1683	GTT/ATC	V/I	ns
7411	B	5049	T	C	4883	27.6	1683	GTT/ATC	V/I	ns
7609	B	5247	A	G	86797	42.5	1749	GAA/GAG	E/E	s
7736	B	5374	T	C	91060	20.4	1792	TTC/CTC	F/L	ns
8027	B	5665	T	G	15944	41.1	1889	TCA/GCA	S/A	ns
8134	B	5772	G	A	29537	28.6	1924	CTG/CTA	L/L	s
8173	B	5811	A	G	68937	43.7	1937	CAA/CAG	Q/Q	s
8269	B	5907	T	C	142467	49.8	1969	CCT/CCC	P/P	s
8320	B	5958	C	T	144467	30.2	1986	GAC/GAT	D/D	s

8356	B	5994	C	T	179879	34.9	1998	TTC/TTT	F/F	s
8362	B	6000	A	G	166225	33.4	2000	GAA/GAG	E/E	s
8370	B	6008	A	G	176602	28.9	2003	GAA/GGA	E/G	ns
8405	B	6043	T	C	294965	32.3	2015	TTA/CTA	L/L	s
8473	B	6111	T	C	204164	36.7	2037	ACT/ACC	T/T	s
8482	B	6120	G	A	224549	35.9	2040	CCG/CCA	P/P	s
8552	B	6190	A	G	211326	35.4	2064	AAA/GAA	K/E	ns
8580	B	6218	A	G	224822	30.7	2073	AAG/AGG	K/R	ns
8638	B	6276	G	T	74838	23.4	2092	TCG/TCT	S/S	s
8825	B	6463	T	C	49943	35.4	2155	TTG/CTG	L/L	s
8927	B	6565	C	T	17701	36.0	2189	CTG/TTG	L/L	s
8977	B	6615	G	A	40769	45.9	2205	CGG/CGA	R/R	s
9037	B	6675	G	A	20134	47.4	2225	CAG/CAA	Q/Q	s
9112	B	6750	A	G	18403	35.2	2250	AGA/AGG	R/R	s
9310	B	6948	T	C	50664	24.1	2316	GAT/GAC	D/D	s
9331	B	6969	A	C	56393	37.6	2323	ATA/ATC	I/I	s
9355	B	6993	A	G	65733	23.6	2331	CAA/CAG	Q/Q	s
9361	B	6999	T	C	69445	42.6	2333	TTT/TTC	F/F	s
9412	B	7050	A	G	84288	39.2	2350	AAA/AAG	K/K	s
9508	B	7146	T	C	24912	29.9	2382	GCT/GCC	A/A	s
9517	B	7155	T	C	19950	33.0	2385	AAT/AAC	N/N	s
9544	B	7182	A	G	22938	25.2	2394	GTA/GTG	V/V	s
9559	B	7197	C	T	33481	41.9	2399	CGC/CGT	R/R	s
9649	B	7287	A	G	63115	35.9	2429	CAA/CAG	Q/Q	s
9661	B	7299	G	A	64715	35.5	2433	AAG/AAA	K/K	s
9859	B	7497	C	T	328569	33.7	2499	GGC/GGT	G/G	s
10120	B	7758	G	A	82174	38.5	2586	CGG/CGA	R/R	s
10195	B	7833	T	C	96786	41.6	2611	CGT/CGC	R/R	s
10219	B	7857	G	A	118742	27.7	2619	CTG/CTA	L/L	s
10303	B	7941	C	T	174294	42.4	2647	CAC/CAT	H/H	s

10414	B	8052	C	T	121899	22.0	2684	ATC/ATT	I/I	s
10543	B	8181	T	C	48703	42.2	2727	ATT/ATC	I/I	s
10927	B	8565	G	A	149973	41.8	2855	ACG/ACA	T/T	s
11023	B	8661	G	A	26739	40.0	2887	GCG/GCA	A/A	s
11171	B	8809	C	T	5131	28.8	2937	CTG/TTG	L/L	s
11491	B	9129	A	G	40133	43.6	3043	TTA/TTG	L/L	s
11513	B	9151	G	A	86220	31.6	3051	GAA/AAA	E/K	ns
11673	B	9311	C	T	33140	20.5	3104	GCA/GTA	A/V	ns
11734	B	9372	G	A	66139	29.4	3124	GTG/GTA	V/V	s
11749	B	9387	T	C	53617	35.6	3129	GCT/GCC	A/A	s
11903	-	-	C	T	294990	20.1	-	-	-	nc
12186	-	-	G	A	25200	39.8	-	-	-	nc

ORF, open reading frame; SNP, single nucleotide polymorphism; nc, SNP included in a non-coding region; s, synonymous SNP; ns, non-synonymous SNP

Figure captions

Fig. 1. Representative virulent (A) and hypovirulent (B) colonies of *C. parasitica* isolated during the surveys, cultivated for 15 days with a 16-h photoperiod, at 25°C.

Fig. 2. Phylogenetic tree constructed from the analysis of the complete genomes of CHV-1, CHV-2, CHV-3 and CHV-4, as available from Genbank.

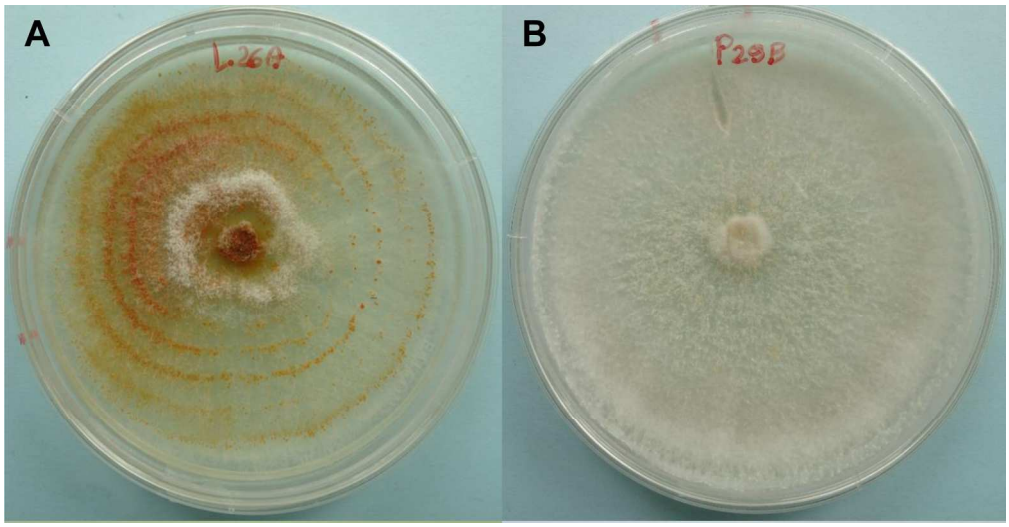

Fig. 1. Representative virulent (A) and hypovirulent (B) colonies of C. parasitica isolated during the surveys, cultivated for 15 days with a 16-h photoperiod, at 25°C.

177x91mm (300 x 300 DPI)

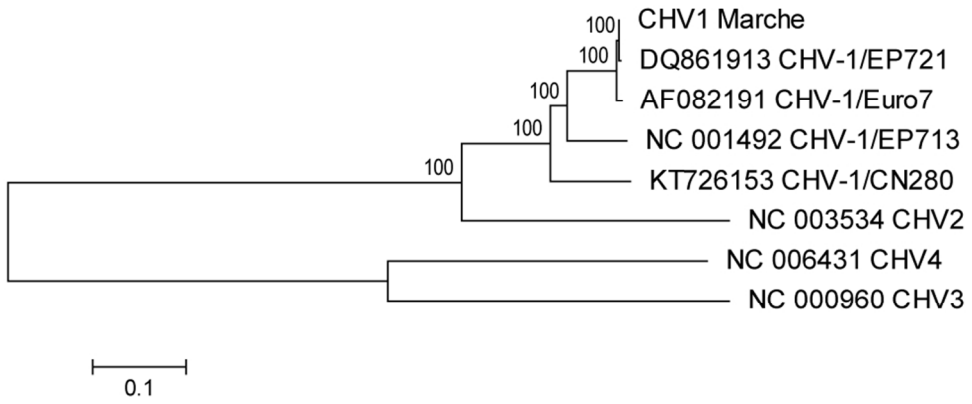

Fig. 2. Phylogenetic tree constructed from the analysis of the complete genomes of CHV-1, CHV-2, CHV-3 and CHV-4, as available from Genbank.

85x34mm (300 x 300 DPI)